IL NUOVO CIMENTO **43 C** (2020) 50
DOI 10.1393/ncc/i2020-20050-3

COLLOQUIA: IFAE 2019

Fermilab Muon $g-2$ experiment: Current status

A. NATH on behalf of the MUON $g-2$ COLLABORATION
INFN, Sezione di Napoli - Napoli, Italy

received 8 June 2020

Summary. — The Muon $g-2$ experiment at Fermilab (E989) is currently measuring the muon magnetic anomaly with a goal precision of 140 part per billion, which will be a fourfold precision improvement over the current best measurement by the previous Muon $g-2$ experiment at the Brookhaven Laboratory (BNL). The BNL-measured value of the muon magnetic anomaly and the corresponding Standard Model (SM) best estimate differ by more than three standard deviation which inspired the current measurement as well as a theoretical drive for a significantly more precise calculation of the muon magnetic anomaly to rule out (or establish) statistical fluctuation as the origin of such a huge discrepancy. Stable central values along with 4-fold precision improvements in both theoretical (SM) and experimental fronts, would imply a $\sim 7\sigma$ discrepancy and that will be a clear hint of the physics beyond the Standard Model. Such an unprecedented precision demands state-of-the-art technological improvements in all involved components to keep the systematic uncertainty below 70 ppb. This paper reports the current status of the E989 experiment after two years of data acquisition.

1. – Introduction

The g-factor is defined as the ratio of the magnetic moment of a particle (charge: e, mass: m) to its angular momentum, weighted by the Larmor ratio ($e/2mc$). For an orbiting electron, g was thought to be 1. When Goudschmit and Uhlenbeck [1] introduced the idea of an intrinsic angular momentum of $h/4\pi$ of the electrons to explain the anomalous *Zeeman* effect, the associated magnetic moment turned out to be exactly double, implying $g = 2$! This value appeared naturally in the low-energy limit of a linear formulation of a Lorentz invariant quantum wave equation by Dirac [2], although Kramers [3] also successfully obtained this value through a classical relativistic formulation of the electron spin. Soon it was realized that g for the electrons must be slightly greater than 2 in order to explain their magnetic moment. Schwinger [4] was the first to calculate the first order correction to the magnetic moment of the electron using QED, the first anomaly calculation. This was the beginning of the QED revolution. Since then, this low-energy observable $g-2$ (g *minus two*), has been playing perhaps the most important role in

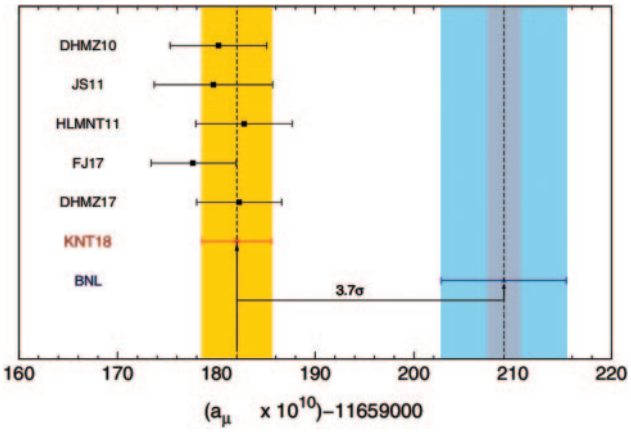

Fig. 1. – The yellow and the sky-blue bands represent the current theoretical (SM) and the experimental world averages of a_μ, respectively. The grey narrow band within the yellow one represents the expected E989 result.

TABLE I. – *Systematic improvements in the new Muon $g-2$ experiment of Fermilab (in ppb).*

Category	E821 uncertainties	E989 improvements	E989 goals
Gain changes	120	Laser calibration system Low-energy threshold	20
Pile-up	80	Low-energy samples recorded Calorimeter segmentation	40
E-field and pitch correction	50	Improved trackers Better storage ring simulations	30

advancing our understanding of the nature around and within us. Lepton's $g-2$ has been providing the most stringent tests of QED specifically and has driven the developement of relativistic local QFT as a theory of the elementary particle physics. The muon being much heavier than the electron and not so short lived, provides the best opportunity to probe new physics ($\sim m_\mu^2/\Lambda^2$). The BNL (E821 experiment) measurement [5], which stands at $\sim 3.5\sigma$ away from the current theoretical (SM) world average (fig. 1), indicates that this might be our window to new physics that is hiding just at the outskirts of the Standard Model. The new Muon $g-2$ experiment (E989) [6] at Fermilab, is aiming for a fourfold precision improvement over the 540 ppb BNL measurement. This requires 20 times more decaying muons and the overall systematic uncertainty must be under 70 ppb. This ambitious goal requires dramatic improvements in several fronts (table I). But before we go into those details, let us first have a brief look at the experimental method.

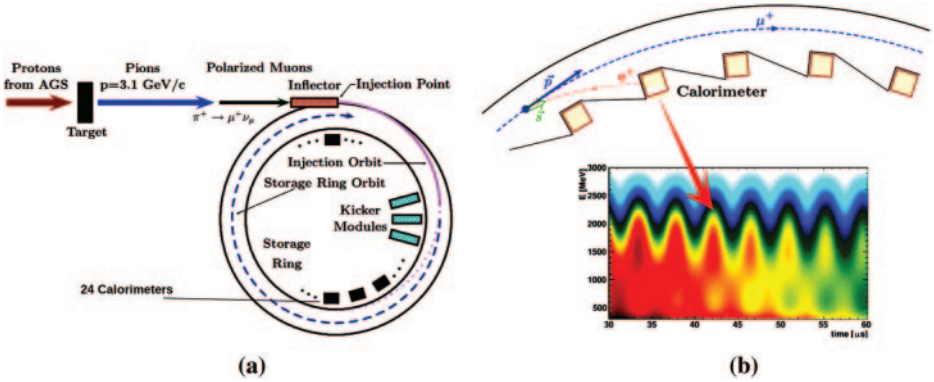

Fig. 2. – (a) Schematic representation of the Muon $g-2$ experiment and (b) when a positron is directed towards the interior of the ring, we see a peak, otherwise a trough.

2. – How do we measure a_μ?

Bunches of highly polarized (spins along the direction of motion) anti-muons are injected (fig. 2(a)) into a magnetic storage ring at a rate of about 11.4 Hz (about 10000 muons per fill). The ring has a diameter of 14 m and produces an exceptionally stable magnetic field of 1.45 T in the muon storage region. Weak interaction prefers positron decays along the direction of the muon spin, and as our beam is highly polarized, those preferred positrons receive more boost and are more energetic than the less preferred ones that decayed opposite to the muon spin. As the muon spin precesses around the magnetic field, so does the direction of emission of these "preferred" high-energy decay positrons. 24 calorimeters evenly spaced inside the ring along the azimuth detect these positrons. When we apply an energy threshold, a modulation in the number of detected positrons (fig. 2(b)) is observed. If the cyclotron and the Larmor frequency were exactly equal, we would not see a modulation though. In the ideal case of muon momenta perpendicular to the magnetic field $\vec{B}$, the difference of these two freuencies can be expressed as

$$\vec{\omega}_a = a_\mu \frac{e\vec{B}}{m_\mu} \tag{1}$$

But for the purpose of vertical beam focussing, electric quadrupoles are used that introduce an electric field term:

$$\vec{\omega}_a = -\frac{e}{m_\mu}\left[a_\mu \vec{B} + \left(a_\mu - \frac{1}{\gamma^2-1}\right)\frac{\vec{\beta}\times\vec{E}}{c}\right]. \tag{2}$$

To eliminate this complication, we choose the *magic momentum*, muons with momenta 3.09 GeV/c, which leads to a cancellation of the $\vec{E}$-field term. The wiggle observed by the calorimeter as shown in fig. 2(b) can then be fitted, in ideal situation, using a function of the form

$$f(t) = Ne^{-t/\tau_\mu}[1 + A\cos(\omega_a + \phi)] \tag{3}$$

and ω_a can be extracted. Here A is the asymmetry, N, the normalization constant and τ_μ, the muon lifetime in the lab frame. In reality, there are several other factors that the analysis team considers for better extraction of the anomalous frequency. This involves the inclusion of effects like *lost muons*, *coherent betatron oscillation* (CBO) etc. The calorimeters are segmented into six rows and nine columns of $25 \times 25 \times 140\,\mathrm{mm}^3$ lead-fluoride (PbF_2) crystals. Each crystal is read out by a single monolithic SiPM. This segmentation reduces the pile-up significantly. A system of straw trackers help reconstruct the decay path and hence also improve the resolution of the calorimeters. But in order to obtain a_μ, a very precise measurement of the magnetic field $\vec{B}$, electronic charge e, and the mass of a muon m_μ, are required. The latter two are known extremely precisely. The magnetic field is measured using pulsed proton NMR probes. There are fixed probes installed inside the ring that measures field at all times, but there is also a trolley probe that runs through the ring when there is no beam.

3. – Design improvements and current status

Table I lists several areas of improvements over the previous E821 experiment. Here we would like to describe one such improvement: the gain correction using a laser-based calibration system [7-10] designed by the Italian Collaboration (INFN). The 24 calorimeters equipped with SiPMs are recording the Cherenkov light emitted by the decay positrons from the muons when passing through the PbF_2 crystals [11]. To achieve the precision goal, it is very important to understand how the gain behaves at various time scales, especially during the muon fill window ($\sim 700\ \mu$s). Consider the equation $r_{e^+}^{Total} = r_{e^+}^{Real} \times G^{SiPM}(t)$, where $r_{e^+}^{Total}$ is the total response of a SiPM to a positron event and $r_{e^+}^{Real}$ is the response that we would see if the gain was stable, and $G^{SiPM}(t)$ is the SiPM gain function. The laser-based calibration system sends laser pulses of known intensity to those calorimeter crystals, both during muon fills as well as outside of them. An array of photodetectors is used to construct a monitoring system consisting of two main parts, the *source monitors* that monitor the intensity of the laser pulses right after they leave the laser heads and *local monitors* that monitor pulses coming back after travelling from the source to the calorimeters. The local monitor also receives a part of the source monitor signal to compare how it changes after travelling the whole optical path of several meters, and it is independent of the gain fluctuation of its photodectector. The third component of the laser system is the *laser control board* [12] that programs the pulse patters. Comparing the SiPM response to the energy detected by the laser monitors, a gain function per calorimeter crystal, that is total of $24 \times 6 \times 9 = 1296$, can be constructed and applied to the measured positron energy to get rid of the systematic uncertainty introduced by the gain variations of the SiPMs. Laser calibration system can also simulate positron events.

Currently we are just entering the Run-3 data acquisition, where several hardware and software improvements have been implemented. Analysis of Run-1 data taking ended in the spring of 2018, and based on data quality cuts, a few data-sets have been selected for the analyses. One such imported golden data-set, the *60 hours* data-set that can lead to a 1.3 ppm ω_a measurement [13], has been analysed by six independent analysis teams. Their data reconstruction, fitting methods and approach, treatments of detector systematics, were all independent. Apart from an absolute blinding of the clocks (a clock shift unknown to all analyzers), another relative blinding by individual groups was applied to their analyses that is known only within a group. In February 2019, unblinding of the second kind happened. All groups came together and lifted the

relative frequency shift, and the results were in perfect agreement within the allowed uncertainty. The consistent results of various analysis groups after the unblinding was a strong proof that all the independent approaches were equally valid and are proceeding in the right direction. Analyses of a few other data quality certified Run-1 data-sets are underway and are expected to be nearing their completion soon. We expect to announce an a_μ based on Run-1 data after rigorous internal review and assesments of systematic uncertaities by the spring of 2020.

* * *

This manuscript has been authored by Fermi Research Alliance, LLC under Contract No. DE-AC02-07CH11359 with the U.S. Department of Energy, Office of Science, Office of High Energy Physics. The research was supported by Istituto Nazionale di Fisica Nucleare (Italy) and by the EU Horizon 2020 Research and Innovation Programme under the Marie Sklodowska-Curie Grant Agreements No. 690835 and No. 734303.

REFERENCES

[1] Uhlenbeck G. E. and Goudsmit S., *Naturwissenchaften*, **13** (1925) 953; *Nature*, **117** (1926) 264.
[2] Dirac P. A. M, *Proc. R. Soc. London A*, **117** (1928) 610.
[3] Kramers H. A., *Physica*, **1** (1934) 182.
[4] Schwinger J., *Phys. Rev.*, **73** (1948) 416.
[5] Bennett G. W. *et al.*, *Phys. Rev. Lett.*, **92** (2004) 161802.
[6] Carey R. M. *et al.*, FERMILAB-PROPOSAL-0989 (2009).
[7] Anastasi A. *et al.*, *Nucl. Instrum. Methods Phys. Res. A*, **788** (2015) 43.
[8] Anastasi A. *et al.*, *JINST*, **13** (2018) T02009.
[9] Anastasi A. *et al.*, *JINST*, **14** (2019) P11025.
[10] Anastasi A. *et al.*, *Nucl. Instrum. Methods Phys. Res. A*, **936** (2019) 372.
[11] Kaspar J. *et al.*, *JINST*, **12** (2017) P01009.
[12] Mastroianni S. *et al.*, *IEEE Trans. Nucl. Sci.*, **64** (2017) 1179.
[13] Fienberg A. T., *The Status and Prospects of the Muon $g-2$ Experiment at Fermilab*, arXiv:1905.05318 [hep-ex].